ELSEVIER

Biochimica et Biophysica Acta 1319 (1997) 69–85

BIOCHIMICA ET BIOPHYSICA ACTA
BBA

The photocycle of bacteriorhodopsin at high pH and ionic strength II. Time-dependent anisotropy studied by partially saturating photoselection

Géza I. Groma [a,*], Roberto A. Bogomolni [b], Walther Stoeckenius [b]

[a] *Institute of Biophysics, Biological Research Centre of Hungarian Academy of Sciences, 6726 Szeged, Hungary*
[b] *Department of Chemistry and Biochemistry, University of California, Santa Cruz, CA 95064, USA*

Received 7 May 1996; accepted 12 September 1996

Abstract

Photoselection measurements with moderate excitation intensity on bacteriorhodopsin (bR) immobilized in a polyacrylamide gel soaked in 3 M KCl in the pH range 8.0–9.5 resulted in an unusual time-dependent anisotropy. In the microsecond region, the anisotropy exhibits a constant level that is considerably less than $2/5$ theoretically expected for the vanishing excitation intensity, indicating partial saturation. In the millisecond region, it becomes time-dependent. Theoretical models for such a time-dependent anisotropy are presented. These models include a consideration of: (i) reorientation of the retinal chromophore during or after excitation, (ii) parallel reactions of differently saturated photoselected species of a heterogenous bR population preexisting in the ground state or photochemically induced, (iii) branching in a photochemical step, and (iv) cooperativity of molecules within a trimer. All of these models describe the anisotropy as a ratio of sums of exponentials, where the rate constants correspond to the kinetics of the photocycle. An analysis of the fitted amplitudes of the exponentials favors the models involving parallel processes rather than those invoking chromophore reorientation.

Keywords: Bacteriorhodopsin; pH; Photoselection; Anisotropy

1. Introduction

In the first paper of this series (this issue), we analyzed the kinetics of the bacteriorhodopsin (bR) photocycle in purple membrane at high ionic strength (3 M KCl) in the pH range 8.0–9.5. We found that the magic angle kinetics at 415 and 550 nm (calculated from absorbances of parallel and perpendicular polarization with respect to the actinic laser flash) can be characterized by seven macroscopic rate constants in the μs–s time range. In this paper, we analyze an unusual time dependence of anisotropy calculated from the same dataset.

In early studies on time-dependent anisotropy at and below the ms region, this phenomenon was attributed to rotational diffusion of the entire protein in the membrane [1–3]. This rotational diffusion was highly restricted or completely eliminated by glutaraldehyde fixation [1,3]. It was a general observation that no transient anisotropy occurred if the purple membrane was immobilized in gel [3–5]. However, Sherman and Caplan [1] reported time-dependent anisotropy even for samples embedded in gel.

* Corresponding author. Fax: +36 62 433133; E-mail: groma@everx.szbk.u-szeged.hu

PII S0005-2728(96)00115-6

The anisotropy changes associated with rotational diffusion are not expected to correlate kinetically with the bR photocycle reactions. It can be expected, however, that photocycle events involving protein and chromophore conformation changes may result in chromophore reorientations and consequently generate synchronous anisotropy changes. According to the C-T model introduced by Fodor et al. [6], a major protein conformational switch takes place on M formation, which relaxes during the N-O-bR steps. It was suggested that this conformational change makes the photocycle irreversible [7]. Recent infrared studies confirmed this basic idea, suggesting a conformational change simultaneously with the M to N transition [8]. Resonance energy-transfer studies [9] indicated a significant change in retinal location between the slow-decaying and fast-decaying intermediates M.

Photoselection measurements on oriented immobilized purple membrane demonstrated that the anisotropy is time-independent from 1 ms to 100 ms [10]. The wavelength dependence of this constant level indicated a 3° difference in the retinal transition dipole moment between the ground and M states of bR. Johnson et al. [11–13] recently reported the occurrence of some reorientation in every phase of the bR photocycle, detected by time-resolved linear dichroism measurements on a purple membrane suspension. They also found that in the ms region the anisotropy changes were markedly reduced in a gel environment.

The majority of the above photoselection studies were carried out at low light intensity and resulted in the theoretically expected value of $2/5$ for the anisotropy [14]. It is well known, however, that saturation during photoselection reduces this value [14–16]. Hence, if several photoselection processes with different degrees of saturation take place on the excitation of bR, they can cause time-dependent anisotropy during the different process of relaxation of photoselected molecules. The recent observation of the intensity dependence of the bR photocycle kinetics indicates that this type of heterogeneity exists in the photocycle [18,19].

The observed transient anisotropy can be caused by chromophore reorientation or by different photoselection processes of partial saturation or both. This paper presents a theoretical analysis of the data in which both phenomena are taken into account. This is an extension of the model of Nagle et al. [15] for the photoselection processes in bR at saturating excitation. In addition, several specific models that predict the different behavior of anisotropy are worked out in detail.

The analysis of the different models presented indicates that photoselection with partial saturation may be an approach to distinguish between kinetic schemes, and is therefore a promising tool for the acquisition of important new information on the bR photocycle.

2. Materials and methods

The dataset used in this paper is identical to that presented in the first part of this series (this issue). Anisotropy was calculated from the measured absorption kinetics via $r = (A_{\|} - A_{\perp})/(A_{\|} + 2A_{\perp})$. The denominator of this expression is proportional to the magic angle absorbance. The exponential fitting of the latter was also described in the former paper. The numerator was fitted with the same time constants by the multilinear regression routine of ASYST (Asyst Software Technologies, Inc., Rochester, New York, USA).

3. Theoretical models of photoselection

3.1. General considerations

Let us consider a photoselection experiment in an XYZ laboratory frame (Fig. 1). The actinic light propagates along the Y axis with vertical (Z axis) polarization. The monitoring beam propagates along the X axis with vertical and horizontal polarization. The orientation of a single molecule during the actinic pulse can be

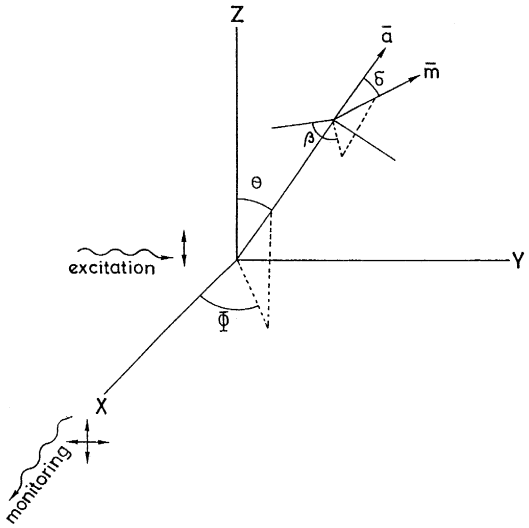

Fig. 1. Laboratory and molecular coordinate systems for the description of photoselection processes.

characterized by a unit vector of absorption moment **a**. It has polar and azimuthal angles Θ and Φ in the *XYZ* frame. The molecules are randomly oriented over these angles. Let the absorption moment for the monitoring beam be a unit vector **m**. The difference in the direction of **a** and **m** reflects the reorientation of the molecule during or after the excitation process. To describe this reorientation let us define a molecular polar coordinate system with respect to **a**. In this, **m** has a polar and azimuthal angle δ and β. Let us suppose that the system is non-degenerate, i.e., δ has a single definite value, but the molecules are randomly oriented over β. The mathematical description of the photoselection and monitoring process is identical to that published for fluorescence anisotropy [17]. Hence, the isotropically averaged absorption monitored with polarization along laboratory axis **j** by molecules excited with polarization along axis **i** will be

$$A_{\mathbf{ij}} = \frac{1}{8\pi^2}\int_0^{2\pi}\int_0^{2\pi}\int_0^{\pi} M_{a\mathbf{i}}^2 M_{m\mathbf{j}}^2 \sin\Theta \, \mathrm{d}\Theta \, \mathrm{d}\Phi \, \mathrm{d}\beta \tag{G.1}$$

where $M_{a\mathbf{i}}^2$ and $M_{m\mathbf{j}}^2$ are the squares of the absorption oscillator components for the actinic and monitoring light projected onto axes **i** and **j**, respectively. For low light intensities:

$$M_{az}^2 = \cos^2\Theta \tag{G.2}$$

$$M_{mz}^2 = \frac{1}{2}\sin^2\Theta\sin^2\delta + \cos^2\Theta\cos^2\delta \tag{G.3}$$

$$M_{my}^2 = \frac{1}{2}\cos^2\Theta\sin^2\Phi\sin^2\delta + \sin^2\Theta\sin^2\Phi\cos^2\delta + \frac{1}{2}\cos^2\Phi\sin^2\delta \tag{G.4}$$

where the random variable β has already been integrated out. Since the intensity of the actinic light in our experiments was moderately high, Eq. (G.2) is not valid. Instead, we will use the generalized form $M_{az}^2 = W^0(I,\cos\Theta)$, where I is the intensity of the actinic light. $W^0(I,\cos\Theta)$ is the angular distribution of photoselected species, called the photoselection weighting function. Its actual form depends on the particular model used to describe the photoprocesses excited by the actinic light.

With the above generalization, when Φ has been integrated out, the absorption of the parallelly and perpendicularly polarized monitoring beams by the excited molecules can be expressed as

$$A_{\parallel} = A_{zz} = \frac{1}{2}\int_{-1}^{+1} W^0(I,\cos\Theta)\left[\frac{1}{2}\sin^2\delta\sin^2\Theta + \cos^2\delta\cos^2\Theta\right]\mathrm{d}\cos\Theta \tag{G.5}$$

$$A_{\perp} = A_{zy} = \frac{1}{2}\int_{-1}^{+1} W^0(I,\cos\Theta)\left[\frac{1}{2}\cos^2\delta\sin^2\Theta + \frac{1}{4}\sin^2\delta(\cos^2\Theta + 1)\right]\mathrm{d}\cos\Theta \tag{G.6}$$

Let us define the averaging functional as

$$AVER[\,f(\cos\Theta)] = \frac{1}{2}\int_{-1}^{+1} W^0(I,\cos\Theta)\,f(\cos\Theta)\,\mathrm{d}\cos\Theta \tag{G.7}$$

and the numerator and denominator of the formula for anisotropy as

$$NUM = A_{\parallel} - A_{\perp} \quad \text{and} \quad DENOM = A_{\parallel} + 2A_{\perp} \tag{G.8}$$

Then, substituting of Eqs. (G.5) and (G.6) into Eq. (G.8), and introduction of the second Legendre polynomial $P_2(x) = (3x^2\text{-}1)/2$, yields

$$NUM = P_2(\cos\delta)\,AVER[\,P_2(\cos\Theta)] \quad \text{and} \quad DENOM = AVER(1) \tag{G.9}$$

With Eq. (G.8), the magic angle absorbance and the anisotropy can be expressed as $A_{mag} = DENOM/3$ and $r = NUM/DENOM$, respectively.

The above formulas are valid for a single initial and excited species of unit extinction coefficient. They can be extended to a mixture of different photoselection processes leading to different series of intermediates. If the pulse length of the actinic flash is much shorter than the life-times of the intermediates, a single intermediate can be characterized by

$$W_{jk}(t) = W_j^0 c_{jk}(t)\,\epsilon_{jk} \tag{G.10}$$

where W_j^0 describes the jth photoselection process, $c_{jk}(t)$ denotes the concentration of the kth intermediate originating from the jth photoselection process at time t, and ϵ_{jk} is its extinction coefficient at the wavelength of the monitoring beam. Since W_j^0 includes the relative concentration of the photoselected molecules at t_0 (i.e., at the end of the actinic flash), $c_{j1}(t_0) = 1$. In our experiments, no rotational diffusion took place due to gel immobilization. Therefore, every intermediate can be characterized by a definite, time-independent δ_{jk}, on the assumption that every chromophore motion is correlated to the photocycle. With the notation $AVER_j$ for the averaging functional with the weighting function W_j^0, the general formulas for the numerator and denominator of the anisotropy will be

$$NUM = \sum_j \sum_k P_2(\cos\delta_{jk})\,AVER_j[\,P_2(\cos\Theta)]\,c_{jk}(t)\,\epsilon_{jk} \tag{G.11}$$

and

$$DENOM = \sum_j \sum_k AVER_j(1)\,c_{jk}(t)\,\epsilon_{jk} \tag{G.12}$$

In Eq. (G.11), the first factor, $P_2(\cos\delta_{jk})$ describes the changes in the orientation of the chromophore or its transition dipole moment in different intermediates. If such a change takes place, it obviously leads to time-dependent anisotropy. The second factor in Eq. (G.11), however, points to another possibility for such a time dependence. If more than one photoselection process takes place with partially saturating excitation, $AVER_j[\,P_2(\cos\Theta)]$ can be different for every j. If these photoselection processes initiate different photocycles, represented by $c_{jk}(t)\epsilon_{jk}$, the anisotropy again becomes time-dependent. Both basic phenomena can be analyzed in the frame of different particular models. In this paper, we discuss several typical specific models in detail. The schemes of the photoprocesses presumed in the different models are outlined in Fig. 2.

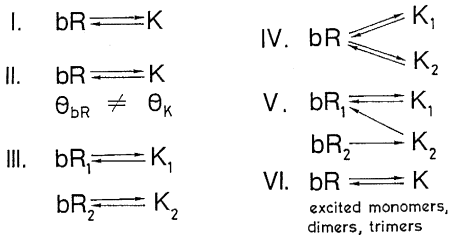

Fig. 2. Schemes of different photoprocesses discussed in Models I–VI.

3.2. Model I. Reorientation of the chromophore after the photoselection process

Let us consider a reversible photoreaction between the bR and K forms. We suppose that the orientation of the transition moment of the chromophore is identical in these forms and changes in the later part of the photocycle. The actinic light is a rectangular pulse with intensity I and duration T. Thus, the differential equation describing the concentration of K during excitation is

$$\frac{\mathrm{d}[K]}{\mathrm{d}t} = I\cos^2\Theta\epsilon_{bR}^a\Phi_{bR}[bR] - I\cos^2\Theta\epsilon_K^a\Phi_K[K] \tag{MI.1}$$

where ϵ_{bR}^a and ϵ_K^a are the absorption coefficients of the bR and K forms at the wavelength of the actinic light, and Φ_{bR} and Φ_K are the quantum efficiencies of the forward and the back photoreaction. (For a clear distinction of the different processes, we have used the notation $[K]$ for the concentration of the intermediate K in photoprocesses and $c_K(t)$ for that in thermal processes.) Let us next suppose that at $t=0$, $[bR]=1$ and $[K]=0$. Nagle et al. [15] analyzed the photoprocesses of this model and found that the photoselection weighting function for the K state is

$$W_K^0 = \frac{f_{bR}}{f_{bR}+f_K}\left[1-\exp(-z\cos^2\Theta)\right] \tag{MI.2}$$

where $f_{bR}=\epsilon_{bR}^a\Phi_{bR}$, $f_K=\epsilon_K^a\Phi_K$ and $z=(f_{bR}+f_K)IT$.

The measured absorption consists of the photocycling signal and the bR depletion-recovery signal. The depletion processes can formally be characterized by a negative concentration $[bR_{depl}]=[bR]-1=-[K]$. This means that the depletion-recovery signal can be described by W_K^0 and the concentration dependence

$$c_{bR}(t) = -\sum_k c_k(t) \tag{MI.3}$$

where the summation over k includes all intermediates. Eqs. (G.11) and (G.12) then reduce to

$$NUM = AVER_K[P_2(\cos\Theta)]\sum_k c_k(t)[\epsilon_k P_2(\cos\delta_k) - \epsilon_{bR}] \tag{MI.4}$$

and

$$DENOM = AVER_K(1)\sum_k c_k(t)(\epsilon_k - \epsilon_{bR}). \tag{MI.5}$$

Nagle et al. [15] showed that with the definitions

$$J_0(z) = \int_0^1 \left[1-\exp(-zx^2)\right]\mathrm{d}x \tag{MI.6}$$

and

$$Q_2(z) = \frac{3}{2}\int_0^1 x^2\left[1-\exp(-zx^2)\right]\mathrm{d}x - \frac{1}{2}J_0(z) \tag{MI.7}$$

the averages in Eqs. (MI.4) and (MI.5) can be expressed as

$$AVER_{\mathrm{K}}(1) = \frac{f_{\mathrm{bR}}}{f_{\mathrm{bR}} + f_{\mathrm{K}}} J_0(z) \tag{MI.8}$$

and

$$AVER_{\mathrm{K}}\left[P_2(\cos\Theta)\right] = \frac{f_{\mathrm{bR}}}{f_{\mathrm{bR}} + f_{\mathrm{K}}} Q_2(z) \tag{MI.9}$$

Here, $(f_{bR})/(f_{bR} + f_K)$ corresponds to the level of complete saturation, $0 < J_0(z) < 1$ is a measure of the degree of saturation, and hence $AVER_K(1)$ is the fraction of molecules in the photocycle [15].

Let us suppose that the time dependence of the concentration of each of the different intermediates is a sum of exponentials:

$$c_{\mathrm{k}}(t) = \sum_l A_{\mathrm{kl}} \exp(-t/\tau_{\mathrm{l}}), \tag{MI.10}$$

where the summation over l includes all exponential terms. Eqs. (MI.5), (MI.8) and (MI.10) then result in the magic angle absorption kinetics:

$$A_{\mathrm{mag}} = \frac{1}{3} \frac{f_{\mathrm{bR}}}{f_{\mathrm{bR}} + f_{\mathrm{K}}} J_0(z) \sum_l \sum_k A_{\mathrm{kl}}(\epsilon_{\mathrm{k}} - \epsilon_{\mathrm{bR}}) \exp(-t/\tau_{\mathrm{l}}) \tag{MI.11}$$

and Eqs. (MI.4), (MI.5), (MI.8), (MI.9) and (MI.10) result in the anisotropy:

$$r = \frac{Q_2(z) \sum_l \sum_k A_{\mathrm{kl}}\left[\epsilon_{\mathrm{k}} P_2(\cos\delta_{\mathrm{k}}) - \epsilon_{\mathrm{bR}}\right] \exp(-t/\tau_{\mathrm{l}})}{J_0(z) \sum_l \sum_k A_{\mathrm{kl}}(\epsilon_{\mathrm{k}} - \epsilon_{\mathrm{bR}}) \exp(-t/\tau_{\mathrm{l}})} \tag{MI.12}$$

An important feature of Eq. (MI.12) is that the time-dependent and light intensity-dependent factors are well separated. (Light intensity is represented via the variable z.) For a closer insight into the intensity dependency, let us consider the following power expansions:

$$J_0(z) = \frac{z}{3} - \frac{z^2}{10} + \frac{z^3}{42} - \frac{z^4}{216} + \ldots, \tag{MI.13}$$

$$Q_2(z) = \frac{2z}{15} - \frac{2z^2}{35} + \frac{z^3}{63} - \frac{z^4}{297} + \ldots, \tag{MI.14}$$

$$\frac{Q_2(z)}{J_0(z)} = \frac{2}{5} - \frac{9z}{175} + \frac{19z^2}{5250} + \frac{72z^3}{336875} + \ldots \tag{MI.15}$$

Eq. (MI.15) gives the well-known value of $2/5$ for the zero intensity limit of the anisotropy level. It is noteworthy that, because of the above-mentioned separation, Eq. (MI.12) indicates a time-dependent anisotropy even at this limit. The graphical representations of $J_0(z)$ (the degree of saturation) and $Q_2(z)/J_0(z)$ (the intensity-dependent factor of anisotropy) are demonstrated in Fig. 3.

3.3. Model II. Reorientation of the chromophore during the photoselection process

Let us suppose that the chromophore changes its orientation or transition dipole moment in the K state by an angle δ. In a molecular coordinate system with respect to the bR state the molecules in the K state are randomly oriented over an azimuthal angle β (Fig. 1). Reorientation takes place not in the later intermediates, but in the recovery of the bR form. All other conditions are identical to those in Model I. This model was fully described

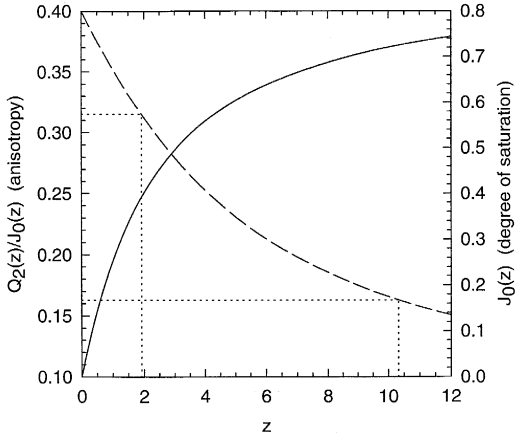

Fig. 3. Light intensity dependence of the degree of saturation ($J_0(z)$, solid line) and anisotropy ($Q_2(z)/J_0(z)$, dashed line) for the simplest saturation model (Model I with zero angle of reorientation). The dimensionless quantity z, proportional to the light intensity, is defined in Eq. (MI.2). The dotted cursors point to the values of $Q_2(z)/J_0(z)$ equal to the amplitude ratios p_4 and p_5 given in Table 1 (averaged over different pH values), calculated from data obtained in CHES buffer at 415 nm. For details, see the analysis of Model III in Section 4.

by Nagle et al. [15]; here, we refer to their main results with our notations.

The orientations of the molecules in the bR and K states in the laboratory frame can be characterized by polar angles Θ and Θ', respectively, for which

$$\cos\Theta' = \cos\Theta\cos\delta + \cos\beta\sin\Theta\sin\delta \tag{MII.1}$$

With the notations of Model I and $q = \cos^2\Theta'/\cos^2\Theta$, the photoselection weighting function of the bR depletion-recovery signal can be expressed as

$$W^0_{\mathrm{bR}} = -\frac{f_{\mathrm{bR}}}{f_{\mathrm{bR}} + qf_K}\left\{1 - \exp\left[-(f_{\mathrm{bR}} + qf_K)\,IT\cos^2\Theta\right]\right\} \tag{MII.2}$$

Functions with the argument of $\cos\Theta$ can be weighted by this expression. The corresponding weighting function of the photocycling signal is $W^0_K = -W^0_{bR}$. This, however, can be used as weighting factor for functions with the argument of $\cos\Theta'$. Since these weighting functions depend not only on $\cos\Theta$, but also on β (via q and $\cos\Theta'$), the averaging functional has to be extended for double integration as

$$DAVER\left[f(\cos\Theta,\beta)\right] = \frac{1}{4\pi}\int_{-1}^{+1}\int_0^{2\pi} W(I,\cos\Theta,\beta)\,f(\cos\Theta,\beta)\,\mathrm{d}\beta\,\mathrm{d}\cos\Theta \tag{MII.3}$$

These averages can be integrated numerically. We next define the averages over W^0_K and W^0_{bR} as

$$G = DAVER_K\left[P_2(\cos\Theta')\right], \quad G' = DAVER_K\left[P_2(\cos\Theta)\right] \tag{MII.4}$$

and

$$H = DAVER_K(1). \tag{MII.5}$$

With these notations, the final formula for the anisotropy will be

$$r = \frac{\sum_l \sum_k (G\epsilon_{\mathrm{k}} - G'\epsilon_{\mathrm{bR}})\,A_{\mathrm{kl}}\exp(-t/\tau_{\mathrm{l}})}{\sum_l \sum_k H(\epsilon_{\mathrm{k}} - \epsilon_{\mathrm{bR}})\,A_{\mathrm{kl}}\exp(-t/\tau_{\mathrm{l}})} \tag{MII.6}$$

The magic angle absorption kinetics is $1/3$ of the denominator of Eq. (MII.6).

If the back-reaction is neglected, the weighting function in Eq. (MII.2) does not depend on β. In this case

$$DAVER_K\left[P_2(\cos\Theta')\right] = P_2(\cos\delta)\,AVER_K\left[P_2(\cos\Theta)\right] \tag{MII.7}$$

and the formula for the anisotropy and magic angle kinetics will be identical to that in Model I for a chromophore reorientation in the K form. Change of the order of summation in Eq. (MII.6) clearly reveals that, as for the previous model, the time-dependent and intensity-dependent factors are separated, leading to time-dependent anisotropy even at the zero intensity limit.

3.4. Model III. Two (or more) photoselection processes due to the coexistence of different bR species

Let us presume the existence of two bR species with different optical and kinetic parameters. Both bR forms have a reversible photoreaction with their own K forms. This leads to two parallel photocycles which do not cross each other. No reorientation of the chromophores takes place. In this case, Eqs. (G.11) and (G.12) reduce to

$$NUM = \sum_{j=1}^{2} AVER_j\left[P_2(\cos\Theta)\right] \sum_k c_{\mathrm{jk}}(t)(\epsilon_{\mathrm{jk}} - \epsilon_{\mathrm{jbR}}) \tag{MIII.1}$$

and

$$DENOM = \sum_{j=1}^{2} AVER_j(1) \sum_k c_{\mathrm{jk}}(t)(\epsilon_{\mathrm{jk}} - \epsilon_{\mathrm{jbR}}) \tag{MIII.2}$$

Let us suppose that n_1 molecules exist in the bR_1 form and n_2 in the bR_2 form. With the same notations as in Model I, we define

$$G_{\mathrm{j}} = AVER_{\mathrm{j}}\left[P_2(\cos\Theta)\right] = n_{\mathrm{j}} \frac{f_{\mathrm{jbR}}}{f_{\mathrm{jbR}} + f_{\mathrm{jK}}} Q_2(z_{\mathrm{j}}) \tag{MIII.3}$$

and

$$H_{\mathrm{j}} = AVER_{\mathrm{j}}(1) = n_{\mathrm{j}} \frac{f_{\mathrm{jbR}}}{f_{\mathrm{jbR}} + f_{\mathrm{jK}}} J_0(z_j) \tag{MIII.4}$$

The anisotropy will then be

$$r = \frac{G_1 \sum_l \sum_k (\epsilon_{1k} - \epsilon_{1bR})\, A_{1kl} \exp(-t/\tau_{1l}) + G_2 \sum_l \sum_k (\epsilon_{2k} - \epsilon_{2bR})\, A_{2kl} \exp(-t/\tau_{2l})}{H_1 \sum_l \sum_k (\epsilon_{1k} - \epsilon_{1bR})\, A_{1kl} \exp(-t/\tau_{1l}) + H_2 \sum_l \sum_k (\epsilon_{2k} - \epsilon_{2bR})\, A_{2kl} \exp(-t/\tau_{2l})} \tag{MIII.5}$$

Again, the magic angle absorption kinetics is $1/3$ of the denominator of Eq. (MIII.5). This model can be extended to more bR forms simply by adding further terms to the numerator and denominator of Eq. (MIII.5).

In contrast with the two previous models, in Eq. (MIII.5), the time-dependent and intensity-dependent factors cannot be separated. Schematically, the structure of Eq. (MIII.5) is the following:

$$r = \frac{Q_2(a_1 I) f_1(t) + Q_2(a_2 I) f_2(t)}{J_0(a_1 I) f_1(t) + J_0(a_2 I) f_2(t)} \tag{MIII.6}$$

where the actual forms of the constants a_1 and a_2 and functions $f_1(t)$ and $f_2(t)$ can be substituted from Eqs. (MIII.3), (MIII.4) and (MIII.5) and the definition of variable z in Eq. (MI.2). The difference in the degrees of saturation corresponding to the two species is represented by the different values of a_1 and a_2 in the arguments of $J_0(z)$ and $Q_2(z)$. To derive the zero intensity limit of the anisotropy, we substitute the first-order terms of the power expansions of $J_0(z)$ (Eq. (MI.13)) and $Q_2(z)$ (Eq. (MI.14)) into Eq. (MIII.6). This yields a time-indepen-

dent value of $2/5$. Hence, in contrast with the two previous models, this model (and also the subsequent ones) predicts time-dependent anisotropy only in the event of partial saturation. (Another criterion of time dependency is the difference in the kinetics of the two corresponding photocycles, as is clear from Eq. (MIII.5).)

3.5. Model IV. Two photoselection processes due to a branching in the photoreaction

Let us suppose that a single bR form has two parallel photoproducts, K_1 and K_2. Both branches of the photoreaction are reversible. K_1 and K_2 initiate their own photocycles. They never cross each other, but terminate in the common bR form. No chromophore reorientation takes place.

The differential equation system for this model is

$$\frac{d[K_1]}{dt} = I\cos^2\Theta\epsilon^a_{bR}\Phi_{1bR}[bR] - I\cos^2\Theta\epsilon^a_{1K}\Phi_{1K}[K_1] \quad \text{(MIV.1)}$$

$$\frac{d[K_2]}{dt} = I\cos^2\Theta\epsilon^a_{bR}\Phi_{2bR}[bR] - I\cos^2\Theta\epsilon^a_{2K}\Phi_{2K}[K_2] \quad \text{(MIV.2)}$$

where the notations are the same as in Model I, ϵ^a_{1K} and ϵ^a_{2K} are the extinction coefficients of K_1 and K_2, respectively, at the wavelength of the actinic light, Φ_{1bR} and Φ_{2bR} are the quantum efficiencies of the phototransitions from bR to K_1 and K_2, respectively, and Φ_{1K} and Φ_{2K} are the quantum efficiencies of the corresponding back photoreactions. The initial conditions $[K_1]=0$, $[K_2]=0$ and $[bR]=1$ at $t=0$ imply $[bR]=1-[K_1]-[K_2]$. Let us define

$$f_{1bR}=\epsilon^a_{bR}\Phi_{1bR} \quad f_{2bR}=\epsilon^a_{bR}\Phi_{2bR} \quad f_{1K}=\epsilon^a_{1K}\Phi_{1K} \quad f_{2K}=\epsilon^a_{2K}\Phi_{2K} \quad \text{(MIV.3)}$$

$$D=\left[(f_{1bR}-f_{2bR}+f_{1K}-f_{2K})^2+4f_{1br}f_{2bR}\right]^{\frac{1}{2}} \quad \text{(MIV.4)}$$

$$C_1=\frac{f_{1bR}f_{2K}}{f_{1bR}f_{2K}+f_{2bR}f_{1K}+f_{1K}f_{2K}} \quad \text{(MIV.5)}$$

$$C_2=\frac{f_{2bR}f_{1K}}{f_{1bR}f_{2K}+f_{2bR}f_{1K}+f_{1K}f_{2K}} \quad \text{(MIV.6)}$$

$$F_1=\left[C_1(f_{1bR}-f_{2bR}+f_{1K}-f_{2K})+2C_2f_{1bR}\right]/2D \quad \text{(MIV.7)}$$

$$F_2=\left[C_2(f_{1bR}-f_{2bR}+f_{1K}-f_{2K})-2C_1f_{2bR}\right]/2D \quad \text{(MIV.8)}$$

$$z^+=\frac{1}{2}(f_{1bR}+f_{2bR}+f_{1K}+f_{2K}+D)IT \quad \text{(MIV.9)}$$

$$z^-=\frac{1}{2}(f_{1bR}+f_{2bR}+f_{1K}+f_{2K}-D)IT \quad \text{(MIV.10)}$$

$$A_1^+=\frac{C_1}{2}+F_1 \quad A_1^-=\frac{C_1}{2}-F_1 \quad A_2^+=\frac{C_2}{2}-F_2 \quad A_2^-=\frac{C_2}{2}+F_2 \quad \text{(MIV.11)}$$

The photoselection weighting functions of K_1 and K_2 will then be

$$W_1^0=A_1^+\left[1-\exp(-z^+\cos^2\Theta)\right]+A_1^-\left[1-\exp(-z^-\cos^2\Theta)\right] \quad \text{(MIV.12)}$$

and

$$W_2^0=A_2^+\left[1-\exp(-z^+\cos^2\Theta)\right]+A_2^-\left[1-\exp(-z^-\cos^2\Theta)\right] \quad \text{(MIV.13)}$$

With the definitions

$$G_j = AVER_j\left[P_2(\cos\Theta)\right] = A_j^+ Q_2(z^+) + A_j^- Q_2(z^-) \tag{MIV.14}$$

and

$$H_j = AVER_j(1) = A_j^+ J_0(z^+) + A_j^- J_0(z^-) \tag{MIV.15}$$

$j = 1, 2$, the formula for the anisotropy is formally identical to Eq. (MIII.5). It should be noted, however, that the intensity dependences of G_1, G_2, H_1 and H_2 are different in the two models.

3.6. Model V. Two photoselection processes due to photochemically induced heterogeneity in the bR conformation

This model was originally suggested by Birge et al. [20]. Let us suppose that in the dark only a single bR form exists (bR_2 in the original notation). Light converts it to a K_2 form. The back photoreaction of K_2 leads not to recovery of the original bR_2, but to a bR_1 form with a slightly different conformation and different optical properties. Light converts bR_1 to its own photoproduct K_1. The back photoreaction of K_1 results in the recovery of bR_1, but not bR_2. K_1 and K_2 start their own (non-crossing) photocycles. The possible thermal back-reaction from bR_1 to bR_2 is negligible during the actinic light pulse. No chromophore reorientation takes place.

The differential equation system for this model is

$$\frac{\mathrm{d}[bR_2]}{\mathrm{d}t} = -I\cos^2\Theta\epsilon^a_{2bR}\Phi_{2bR}[bR_2] \tag{MV.1}$$

$$\frac{\mathrm{d}[K_2]}{\mathrm{d}t} = I\cos^2\Theta\epsilon^a_{2bR}\Phi_{2bR}[bR_2] - I\cos^2\Theta\epsilon^a_{2K}\Phi_{2K}[K_2] \tag{MV.2}$$

$$\frac{\mathrm{d}[K_1]}{\mathrm{d}t} = I\cos^2\Theta\epsilon^a_{1bR}\Phi_{1bR}[bR_1] - I\cos^2\Theta\epsilon^a_{1K}\Phi_{1K}[K_1] \tag{MV.3}$$

where the notations are the same as in Model I, ϵ^a_{1bR}, ϵ^a_{2bR}, ϵ^a_{1K} and ϵ^a_{2K} are the extinction coefficients of bR_1, bR_2, K_1 and K_2, respectively, at the wavelength of the actinic light, Φ_{1bR} and Φ_{2bR} are the quantum efficiencies of the phototransitions from bR_1 to K_1 and bR_2 to K_2, respectively, and Φ_{1K} and Φ_{2K} are the quantum efficiencies of the back photoreactions from K_1 to bR_1 and from K_2 to bR_1, respectively. The initial conditions $[bR_1] = 0$, $[K_1] = 0$, $[K_2] = 0$ and $[bR_2] = 1$ at $t = 0$ imply $[bR_1] = 1\text{-}[bR_1]\text{-}[K_1]\text{-}[K_2]$. Let us define

$$f_{1bR} = \epsilon^a_{1bR}\Phi_{1bR} \quad f_{2bR} = \epsilon^a_{2bR}\Phi_{2bR} \quad f_{1K} = \epsilon^a_{1K}\Phi_{1K} \quad f_{2K} = \epsilon^a_{2K}\Phi_{2K} \tag{MV.4}$$

$$A_1^1 = \frac{f_{1bR} f_{2bR} f_{2K}}{(f_{1bR} + f_{1K})(f_{1bR} + f_{1K} - f_{2bR})(f_{1bR} + f_{1K} - f_{2K})} \tag{MV.5}$$

$$A_1^2 = \frac{f_{1bR} f_{2bR}}{(f_{2K} - f_{2bR})(f_{1bR} + f_{1K} - f_{2K})} \tag{MV.6}$$

$$A_1^3 = \frac{f_{1bR} f_{2K}}{(f_{2K} - f_{2bR})(f_{1bR} + f_{1K} - f_{2bR})} \tag{MV.7}$$

$$A_2 = \frac{f_{2bR}}{f_{2K} - f_{2bR}} \tag{MV.8}$$

$$z_1 = (f_{1bR} + f_{1K})IT \quad z_2^1 = f_{2K}IT \quad z_2^2 = f_{2bR}IT \tag{MV.9}$$

The photoselection weighting functions of K_1 and K_2 will then be

$$W_1^0 = A_1^1\left[1 - \exp\left(-z_1\cos^2\Theta\right)\right] - A_1^2\left[1 - \exp\left(-z_2^1\cos^2\Theta\right)\right] + A_1^3\left[1 - \exp\left(-z_2^2\cos^2\Theta\right)\right] \quad \text{(MV.10)}$$

and

$$W_2^0 = A_2\left[1 - \exp\left(-z_2^1\cos^2\Theta\right)\right] - A_2\left[1 - \exp\left(-z_2^2\cos^2\Theta\right)\right] \quad \text{(MV.11)}$$

With the definitions

$$G_1 = AVER_1\left[P_2(\cos\Theta)\right] = A_1^1 Q_2(z_1) - A_1^2 Q_2\left(z_2^1\right) + A_1^3 Q_2\left(z_2^2\right) \quad \text{(MV.12)}$$

$$G_2 = AVER_2\left[P_2(\cos\Theta)\right] = A_2\left[Q_2\left(z_2^1\right) - Q_2\left(z_2^2\right)\right] \quad \text{(MV.13)}$$

$$H_1 = AVER_1(1) = A_1^1 J_0(z_1) - A_1^2 J_0\left(z_2^1\right) + A_1^3 J_0\left(z_2^2\right) \quad \text{(MV.14)}$$

$$H_2 = AVER_2(1) = A_2\left[J_0\left(z_2^1\right) - J_0\left(z_2^2\right)\right] \quad \text{(MV.15)}$$

the formula for the anisotropy will again be identical to Eq. (MIII.5). The intensity dependences of G_1, G_2, H_1 and H_2 are different from those in Models III and IV.

3.7. Model VI. Two (or three) photoselection processes due to the cooperativity among bR molecules within a trimer

Let us presume that cooperativity affects not the photoprocesses, but the later steps of the photocycle. The kinetics of the photocycle depends on whether the cycling molecules within a trimer are in the monomeric, dimeric or trimeric state [21]. No chromophore reorientation takes place. Everything else is identical to that described in Model I. The total photoselection weighting function, which is equal to the total fraction cycling with angle Θ, is then identical to that determined by Eq. (MI.2):

$$W = s\left[1 - \exp(-z\cos^2\Theta)\right] \quad \text{(MVI.1)}$$

where $s = f_{bR}/(f_{bR} + f_K)$. According to the model of Ohno et al. [21], the fractions cycling in the monomeric, dimeric and trimeric states with angle Θ are

$$W_M = W - 2W^2 + W^3, \quad W_D = 2W^2 - 2W^3 \quad \text{and} \quad W_T = W^3 \quad \text{(MVI.2)}$$

respectively. Other cooperativity models can be described in a similar manner [22]. The averages of these weighting functions can be expressed as

$$AVER_M(1) = (s - 4s^2 + 3s^3)J_0(z) + (2s^2 - 3s^3)J_0(2z) + s^3 J_0(3z) \quad \text{(MVI.3)}$$

$$AVER_D(1) = (4s^2 - 6s^3)J_0(z) + (6s^3 - 2s^2)J_0(2z) - 2s^3 J_0(3z) \quad \text{(MVI.4)}$$

$$AVER_T(1) = 3s^3 J_0(z) - 3s^3 J_0(2z) + s^3 J_0(3z) \quad \text{(MVI.5)}$$

Averages for $P_2(\cos\Theta)$ can be obtained by replacing $J_0(x)$ with $Q_2(x)$ in Eqs. (MV.3), (MV.4) and (MV.5). It is assumed for simplicity that the photocycles in the dimeric and trimeric states are identical, but differ from that in the monomeric state. Then with the definitions

$$G_1 = AVER_M\left[P_2(\cos\Theta)\right] \quad \text{(MVI.6)}$$

$$G_2 = AVER_D\left[P_2(\cos\Theta)\right] + AVER_T\left[P_2(\cos\theta)\right] \quad \text{(MVI.7)}$$

$$H_1 = AVER_M(1) \quad \text{(MVI.8)}$$

$$H_2 = AVER_D(1) + AVER_T(1) \quad \text{(MVI.9)}$$

the formula for the anisotropy will again be identical to Eq. (MIII.5). The intensity dependences of G_1, G_2, H_1 and H_2 are different from those in Models III, IV and V.

The above formulas are strictly valid only if the individual chromophores within a trimer are parallel. In the real case, however, the chromophores display a 3-fold symmetry with an angle δ between neighboring molecules. The consequence of this is that Eq. (MVI.1) is valid only for an individual observed molecule. The weighting functions of its neighbors within the trimer are

$$W' = s\left[1 - \exp(-z\cos^2\Theta')\right] \tag{MVI.10}$$

and

$$W'' = s\left[1 - \exp(-z\cos^2\Theta'')\right] \tag{MVI.11}$$

where the additional polar angles Θ' and Θ'' can be handled as in Model II, i.e., $\cos\Theta'$ is determined by Eq. (MII.1), while

$$\cos\Theta'' = \cos\Theta\cos\delta + \cos(\beta + \alpha)\sin\Theta\sin\delta \tag{MVI.12}$$

where $\cos\alpha = \cos\delta/(1 + \cos\delta)$. The modified weighting functions of the monomeric, dimeric and trimeric photocycling states are then

$$W_M = W - WW' - WW'' + WW'W'' \tag{MVI.13}$$

$$W_D = WW' + WW'' - 2WW'W'' \tag{MVI.14}$$

and

$$W_T = WW'W'' \tag{MVI.15}$$

respectively. Averages with these modified weighting functions can be calculated numerically by using double integration according to Eq. (MII.3).

4. Results and discussion

Typical time dependences of the anisotropy at 415 and 550 nm are presented in Fig. 4. In the microsecond time domain, these have a constant level, which is much lower than the theoretical value of $2/5$ for a low-intensity photoselection process. This level is further decreased in the millisecond region. At about 100 ms, it definitely increases again at 550 nm, while at 415 nm this region is uncertain due to the increased statistical

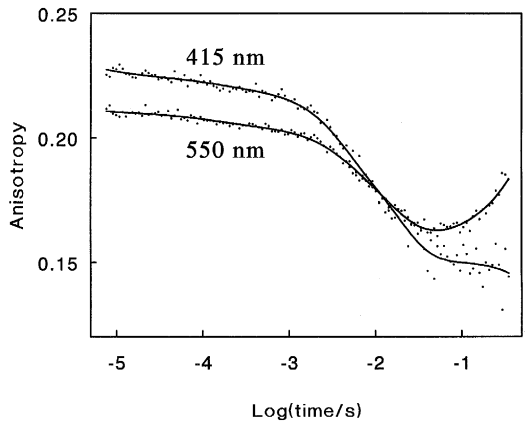

Fig. 4. Dotted line: Time dependence of the anisotropy of bacteriorhodopsin immobilized in 15% polyacrylamide gel and soaked in 3 M KCl, 100 mM CHES buffer, pH = 9.5 at 20°C, monitored at 415 and 550 nm. Solid line: Anisotropy calculated by fitting the experimentally determined numerator and denominator of its formula (see Eq. (G.8)) with the sum of seven exponentials. The rate constants used in the fit are equivalent to those determined for magic angle absorption kinetics. For details of the experimental procedure and the fitting methods, see the first paper of this series (this issue) and Section 2.

error. These overall tendencies are common in the studied pH range of 8.0–9.5 in both CHES and borate buffers, although the changes are somewhat more pronounced at higher pH and in CHES buffer. No similar time dependence of the anisotropy on the gel-immobilized sample was observed in previous photoselection studies [3–5,10,13].

As pointed out in the previous section, the above time dependence of the anisotropy can be explained either by a chromophore reorientation or by the existence of two (or more) photoselection processes with nonlinear intensity dependence. The temporal behavior of the anisotropy is described by Eqs. (MI.12), (MII.6) and (MIII.5) for the different models we analyzed. A common feature of these formulas is that their numerator and denominator consists of a sum of exponential terms of identical time constants but different amplitudes. The denominator is always proportional to the magic angle absorption kinetics. It was shown in the first paper of this series (this issue) that the absorption kinetics at 415 and 550 nm can be characterized by a sum of seven exponentials. According to the above formulas, the experimentally determined numerator of the anisotropy ($I_{\|}$-$I_{\perp}$) should also be fitted with the same time constants. The fitting anisotropy calculated by means of this method is represented by the solid lines in Fig. 4. Clearly, the fitting curves follow the experimental ones very well. This supports our fundamental hypothesis that the kinetics of anisotropy is correlated with the photocycle, and not with rotational diffusion. Hence, the time dependence of the anisotropy can be characterized well by the set of amplitudes in the numerator and the denominator.

To interpret the set of amplitudes determined by the above fitting method, we must consider the following general problem. These amplitudes (and also the corresponding time constants) are macroscopic parameters. Their relations to the real molecular rate parameters depend on the particular model used to describe the scheme of the photocycle [23]. In a general case, these relations are complicated. Although seven components describe our dataset well, this number is more than the number of components in the generally accepted simple photocycle schemes, and hence we cannot use the molecular parameters to be found in the literature. For the same reason, the extinction coefficients attributed to the different components are also unknown, and our data (taken only at two wavelengths) are not sufficiently complete to permit their determination. This problem is manifested in Eqs. (MI.12), (MII.6) and (MIII.5) as a sum over the different intermediates, represented by index k. In the case of Models I and II, the most important parameters to be determined from the experimental anisotropy data are the angles of chromophore reorientation in the different intermediates. These values are incorporated in the sums over k in Eqs. (MI.12) and (MII.6). Hence, they can be determined only in the framework of a particular photocycle model, i.e., in the knowledge of the molecular kinetic and spectral parameters. The situation is somewhat better for Models III, IV, V, and VI. In the common formula of these cases, Eq. (MIII.5), the important parameters G_1, G_2, H_1 and H_2 are out of sums over k, and hence these models can be analyzed more generally.

In a forthcoming paper we will make an attempt to obtain more detailed information about the molecular parameters by fitting them to our whole dataset, similarly as in the method described by Nagle [23]. Here, we will make general conclusions from the partial information which can be gained even in the absence of these parameters. Such useful information can be acquired in the following way. Instead of dividing the complete numerator by the complete denominator in the anisotropy expression, we can separately divide the fitted amplitude of a particular exponential component in the nominator by the corresponding amplitude in the denominator. The ratios calculated in this way for all seven exponential components are listed in Table 1 for pH values of 8.0, 8.5, 9.0 and 9.5 in CHES and borate buffers at monitoring wavelengths of 415 and 550 nm. Table 1 reveals the following general tendencies, valid for each pH value in both buffers:

- The first three components have identical values within statistical error.
- The fourth component at 415 nm has a higher level than the first three. The corresponding value at 550 nm is noninformative because it is completely corrupted by error (it is a ratio of two very small values).
- The fifth component has a lower level than the first three.
- The sixth component (when it is informative) has a value identical to that of the first three.
- The seventh component is noninformative.

Table 1
Component-wise ratios of the amplitudes of the seven exponentials [a] fitted to the experimentally determined numerator and denominator of anisotropy of bR in 3 M KCl, 100 mM CHES and borate buffer of different pH at 20°C, monitored at 415 and 550 nm

pH	p_1	p_2	p_3	p_4	p_5	p_6	p_7
CHES 415 nm							
8.0	0.25	0.26	0.27	0.32	0.19	0.45 [b]	0.20 [b]
8.5	0.23	0.26	0.27	0.33	0.16	0.52 [b]	0.03 [b]
9.0	0.24	0.23	0.25	0.32	0.15	0.14 [b]	0.14 [b]
9.5	0.22	0.21	0.24	0.29	0.15	0.16 [b]	0.12 [b]
CHES 550 nm							
8.0	0.22	0.23	0.24	−0.49 [b]	0.20	0.24	0.22 [b]
8.5	0.24	0.24	0.26	−3.70 [b]	0.21	0.26	0.23 [b]
9.0	0.22	0.21	0.22	−1.60 [b]	0.15	0.24	0.18 [b]
9.5	0.21	0.19	0.21	2.70 [b]	0.14	0.13	0.25 [b]
borate 415 nm							
8.0	0.23	0.24	0.24	0.31	0.21	0.25	0.21 [b]
8.5	0.28	0.26	0.27	0.33	0.21	0.27	0.20 [b]
9.0	0.23	0.23	0.25	0.33	0.19	0.21	0.18 [b]
9.5	0.27	0.25	0.26	0.39	0.22	0.23	0.21 [b]
borate 550 nm							
8.0	0.23	0.25	0.26	0.23 [b]	0.24	0.25	0.29 [b]
8.5	0.27	0.26	0.28	0.21 [b]	0.26	0.28	0.24 [b]
9.0	0.23	0.21	0.23	0.04 [b]	0.19	0.22	0.19 [b]
9.5	0.21	0.22	0.24	−0.25 [b]	0.18	0.21	0.18 [b]

[a] The time constants corresponding to the seven components are presented in Fig. 4 in the first paper of this series (this issue). At pH = 9.0 in CHES buffer, these values are 0.01, 0.2, 2, 10, 80, 300 and 1000 ms, respectively.
[b] These amplitude ratios are noninformative due to high error corruption.

The higher level of the fourth component is not manifested in the plots of Fig. 4. However, our model calculations clearly show that this higher value is absolutely necessary if a curve of the time dependence of anisotropy similar to the experimental one is to be obtained.

The conclusion from the above analysis is that the fourth component has a higher, and the fifth component a lower value than the normal level of the amplitude ratio. This effect will be analyzed in the framework of the different models described in the previous section.

Model I presumes a change in the orientation of the retinal chromophore after the photoprocesses. As stated above, the corresponding formula for the anisotropy, Eq. (MI.12), cannot be used in its general form. Hence, let us consider only the simplest case, supposing a unidirectional, unbranching photocycle, where the decay of every intermediate is much slower than its rise. Every exponential component can then be attributed to a single transition. In this case, the ratio of the amplitudes in the numerator and the denominator for a component corresponding to a transition from intermediate i to intermediate $i+1$ can be expressed from Eq. (MI.12) as

$$p_{i+1} = p_0 \frac{\epsilon_i q_i - \epsilon_{i+1} q_{i+1}}{\epsilon_i - \epsilon_{i+1}} \qquad \text{(R.1)}$$

where $p_0 = Q_2(z)/J_0(z)$ and $q_i = P_2(\cos\delta_i)$.

The normal level of the amplitude ratio can be attributed to the original chromophore orientation, i.e., it corresponds to p_0. This means that, for $i = 0$, 1, 2 and 5, Eq. (R.1) implies $\delta_i = 0$. Consequently, if we assume a reorientation process, it should take place in the transition described by the fourth component ($i = 3$), and in the course of the fifth component ($i = 4$) the chromophore should return to its original position. This model is consistent with the data for $i \le 3$. Since $-1/2 \le P_2(\cos\delta) \le 1$, according to Eq. (R.1), p can have any value. This could explain the increased value of the amplitude ratio of the fourth component ($i = 3$) at 415 nm (unfortunately, the corresponding ratio at 550 nm is noninformative).

Let us consider now what Eq. (R.1) implies for the fifth component ($i = 4$). In this case, $q_{i+1} = 1$ and $p < p_0$; hence, Eq. (R.1) is satisfied for positive extinction coefficients only if $q_i > p/p_0$. This formally gives an upper limit for the angle of chromophore reorientation. The average value calculated from Table 1 for this upper limit is $21 \pm 7°$. However, the real meaning of this value is questionable. For nonzero angle of reorientation, Eq. (R.1) implies a strong wavelength dependence of the corresponding amplitude ratio. This should be especially striking for 415 and 550 nm. Very different extinction coefficients can be expected at these wavelengths for every known bR intermediate. Additionally, we found that at 415 and 550 nm the numerators even have opposite signs. Although this theoretically predicted wavelength dependence is strictly valid only for the above simplified photocycle scheme, it is rather unlikely that in a more complex scheme the wavelength dependence would be completely compensated. Table 1 indicates that the amplitude ratios of the fifth component are well determined and (especially for pH = 8.5 and 9.0) do not exhibit any wavelength dependence beyond statistical error. This contradiction indicates that Model I is probably not valid, i.e., the time dependence of the anisotropy probably cannot be attributed to a chromophore reorientation process after the photoselection. Hence, the angle of reorientation formally calculated above has no real meaning. This is in accordance with the previous photoselection studies, where a time-dependent anisotropy similar to that we found was not observed [3–5,10–13].

In the case of Model II, Eq. (MII.6) also suggests a strong wavelength dependence for the amplitude ratio in the terminal part of the photocycle when the recovery signal mixes with the photocycling signal. Hence, by the above argument we do not favor this model, either.

Models III, IV, V and VI describe parallel photocycles starting from different photoselection processes. These models predict transient anisotropy only in the event of partially saturating photoselection. This feature was explicitly demonstrated for Model III, in the discussion of the structure of Eq. (MIII.5), but it is also valid for the other models in the above category. (The key point is that in all of these models the functions $H(z)$ can be derived from the corresponding functions $G(z)$ by substituting $Q_2(z)$ in place of $J_0(z)$. This ensures that in the first-order approximation the numerator and the denominator in the common anisotropy formula Eq. (MIII.5) differ only in the time-independent factor of $2/5$.) Since the normal level of anisotropy in our experiments is much less than $2/5$ (Table 1), the criterion of partial saturation is satisfied. The above four models differ only in the light intensity dependence of G_1, G_2, H_1 and H_2 in Eq. (MIII.5); hence, for data taken at a single excitation intensity, they can be discussed together. It is to be expected that the two branches of the photocycle are not completely different, but the majority of the intermediates have indistinguishable kinetic and spectroscopic parameters. In these degenerate cases, the component-wise division of the amplitudes in Eq. (MIII.5) results in

$$p_{deg} = \frac{G_1 + G_2}{H_1 + H_2} \tag{R.2}$$

while in nondegenerate cases it results in

$$p_1 = \frac{G_1}{H_1} \quad \text{or} \quad p_2 = \frac{G_2}{H_2} \tag{R.3}$$

These formulas do not depend on the wavelength of observation or on the scheme of the photocycle. (However, the possibility of a special case cannot be excluded: identical time constants with different amplitudes in the two cycles; Eq. (R.2) is then wavelength-dependent.) As a consequence of Eqs. (R.1) and (R.2), the value of p_{deg} falls between p_1 and p_2. Through these features, our data can readily be interpreted by means of these models. According to this interpretation, the two parallel photocycles differ only in one time constant, represented by the fourth and the fifth (nondegenerate) components, with time constants of 10 ms and 80 ms, respectively at pH = 9.0. The normal level of the anisotropy, on the other hand, corresponds to degenerate components.

To examine the previous explanation in a more quantitative manner, let us consider Model III again as a case

study, this being the simplest in this category. In Model III the nondegenerate amplidude ratios can be expressed from Eqs. (MIII.3) and (MIII.4) as

$$p_j = \frac{Q_2(z_j)}{J_0(z_j)} \tag{R.4}$$

reflecting the fact that the different degree of saturation corresponding to the parallelly existing bR species is caused simply by the different values of z. In Fig. 3, the cursors point to the values of z and $Q_2(z)/J_0(z)$ corresponding to p_4 and p_5 according to this model. (Data for CHES buffer and 415 nm observation were taken from Table 1 and are averages of the data at the different pH values.) It is seen that the values of z differ by a factor of five. At a constant light intensity level, this is due to the different values of $\epsilon^a_{bR}\Phi_{bR} + \epsilon^a_K\Phi_K$ for the two bR species (see the definition of z in Eq. (MI.2)). It may be supposed that the extinction coefficients of the different species are roughly identical and the differences rather lie in the quantum efficiencies. For 'normal' bR the quantum efficiencies for both the forward and the reverse photoreaction are very high, and thus it is easy to imagine a 'less effective' version, having quantum efficiencies of five times less. Further, the values of quantum efficiencies are still a matter of controversy (see below).

All the previous calculations were based on the assumption that the excitation of the samples could be characterized by a single, well-defined value of the light intensity. In reality, the samples have relatively high optical density ($OD = 1$ at 570 nm), leading to a gradient of the exciting intensity along the Y-axis (see Fig. 1). Describing this gradient as $I(y)$, the corrected form of Eq. (MIII.5) will be

$$r = \int_0^D \frac{G_1[I(y)]\, f_1(t) + G_2[I(y)]\, f_2(t)}{H_1[I(y)]\, f_1(t) + H_2[I(y)]\, f_2(t)}\, \mathrm{d}y \tag{R.5}$$

where D is the thickness of the sample. This general formula is valid for Models III, IV, V and VI, and the actual forms of functions G_1, G_2, H_1 and H_2 depend on the particular model. Fortunately, the above correction does not introduce any new qualitative feature to the time dependence of the anisotropy. It still will be time-dependent only if the excitation is (at least partially) saturating and $f_1(t)$ is not identical to $f_2(t)$ (i.e., two different photocycles run parallel). On the other hand, the intensity-dependent and the time-dependent terms are no more separable in Eq. (R.5). This means that the actual shape of $r(t)$ is somewhat modified by this correction.

An additional common feaure of the above category of models is that, unlike Models I and II, they predict a light intensity dependence of the magic angle absorption, too (see the denominator of Eq. (MIII.5)). Experimental evidence for such an intensity dependence was published recently [18,19]. There are also indications of the existence of parallel photocycles at alkaline pH [24]. Hence, we favor these types of models rather than presume chromophore reorientation.

The molecular mechanisms leading to the kinetic difference in the corresponding photocycle are completely different for Models III, IV, V and VI. Model III simply supposes that the preparation is heterogenous in bR species. The reality of this possibility is supported by the observation of two bands in the isoelectric focusing profile of a highly purified purple membrane preparation, interpreted as the coexistence of two protein conformers [25]. Branching in the photoreaction of bR (Model IV) is a rarely considered, but very plausible explanation for the origin of parallel photocycles. A closer examination of the primary part of the photocycle would be needed for a decision on this model. The concept of the light-induced heterogeneity of the bR conformation (Model V) was introduced by Birge et al. [20] to explain the controversy concerning the reported quantum efficiencies for the primary photochemical process. More direct experimental evidence has not been found to support this model, and an alternative explanation of the controversy has not been reported, either. Model VI supposes cooperativity among bR, the molecules within a trimer. This is the most favored explanation for the observed intensity dependence of the photocycle kinetics [21,22]. However, a similar intensity dependence is qualitatively expected in the framework of Models III–V, too.

Merely on the basis of the data presented here (i.e., obtained at a single light intensity), it is not possible to distinguish which of the above molecular mechanisms is truly responsible for the observed time-dependent anisotropy. On the other hand, the presented theory combined with a more complete dataset, involving different light intensities, is a powerful tool for selection of the correct model. Experiments to acquire such a dataset were recently carried out [19] and the results are currently undergoing analysis in the framework of the models presented in this paper.

Acknowledgements

Thanks are due to A. Dér and Z. Tokaji for fruitful discussions on the possible photoselection processes of bacteriorhodopsin. This work was supported by National Institute of Health Program Project Grant GM-27507 (W.S. and R.A.B.), NSF Grant DBM-8717193 (R.A.B.), NIH Grant GM-43561 (R.A.B.) and National Scientific Research Foundation of Hungary Grants OTKA T914 and T6401 (G.I.G).

References

[1] Sherman, W.V. and Caplan, S.R. (1977) Nature 265, 273–274.
[2] Cherry, R.J., Heyn, M.P. and Oesterhelt, D. (1977) FEBS. Lett. 78, 25–30.
[3] Ahl, P.L. and Cone, R.A. (1984) Biophys. J. 45, 1039–1049.
[4] Czégé, J., Dér, A., Zimányi, L. and Keszthelyi, L. (1982) Proc. Natl. Acad. Sci. USA 79, 7273–7277.
[5] Dér, A., Száraz, S. and Czégé, J. (1988) Biophys. J. 54, 1175.
[6] Fodor, S.P., Ames, J.B., Gebhard, R., Van der Berg, E.M., Stoeckenius, W., Lugtenburg, J. and Mathies, R.A. (1988) Biochemistry 27, 7097–7101.
[7] Váró, G. and Lanyi, J.K. (1991) Biochemistry 30, 5016–5022.
[8] Ormos, P., Chu, K. and Mourant, J. (1992) Biochemistry 31, 6933–6937.
[9] Hasselbacher, C.A. and Dewey, T.G. (1986) Biochemistry 25, 6236–6243.
[10] Heyn, M.P. and Otto, H. (1992) Photochem. Photobiol. 56, 1105–1112.
[11] Wan, C., Qian, J. and Johnson, C.K. (1991) Biochemistry 30, 394–400.
[12] Wan, C., Qian, J. and Johnson, C.K. (1993) Biophys. J. 65, 927–938.
[13] Song, Q., Harms, G.S., Wan, C. and Johnson, C.K. (1994) Biochemistry 33, 14026–14033.
[14] Kliger, D.S., Lewis, J.W. and Randall, C.E. (1990) Polarized Light in Optics and Spectroscopy, Academic Press, New York, pp. 201–236.
[15] Nagle, J.F., Bhattacharjee, S.M., Parodi, L.A. and Lozier, R.H. (1983) Photochem. Photobiol. 38, 331–339.
[16] Ansari, A. and Szabo, A. (1993) Biophys. J. 64, 838–851.
[17] Chapoy, L.L. and DuPré, D.B. (1978) J. Chem. Phys. 69, 519–524.
[18] Tokaji, Z. and Dancsházy, Z. (1991) FEBS Lett. 281, 170–172.
[19] Tokaji, Z. and Dancsházy, Z. (1992) in Structures and Functions of Retinal Proteins (J.L. Rigaud, ed.), Colloque INSERM/John Libbey Eurotext, Vol. 221, pp. 175–178.
[20] Birge, R.R., Cooper, T.M., Lawrence, A.F., Masthay, M.B., Vasilakis, C., Zhang, C.-F. and Zidovetzki, R. (1989) J. Am. Chem. Soc. 111, 4063–4074.
[21] Ohno, K., Takeuchi, Y. and Yoshida, M. (1981) Photochem. Photobiol. 33, 573–578.
[22] Tokaji, Z. (1993) Biophys. J. 65, 1130–1134.
[23] Nagle, J.F. (1991) Biophys. J. 59, 476–487.
[24] Balashov, S.P., Govindjee, R. and Ebrey, T.G. (1991) Biophys. J. 60, 475–490.
[25] Miercke, L.J.W., Ross, P.E., Stroud, R.M. and Dratz, E.A. (1989) J. Biol. Chem. 264, 7531–7535.